Comparisons Between Array Derived Dynamic Strain Rate and Fiber-optic Distributed Acoustic Sensing Strain Rate

DAS Workshop UW-Madison
June 2023

Gene Ichinose [1], Robert Mellors [2], Justin Barno [1] and Rengin Gok [1]
(1) Lawrence Livermore National Laboratory
(2) UC San Diego | Scripps Institution of Oceanography

LLNL-PRES-849701

This work was performed under the auspices of the U.S. Department of Energy by Lawrence Livermore National Laboratory under contract DE-AC52-07NA27344. Lawrence Livermore National Security, LLC

Lawrence Livermore National Laboratory

Introduction and Motivation

Are strain signals coherent enough to be used for array processing?

- Motivations
  - Seismic arrays are the workhorse of the global seismic monitoring networks
  - can we use fiber-optic DAS for seismic array processing?

- Particle motion is the foundational measurand of most seismological techniques but DAS measures strain rate.
  - What is the relationship between 3C particle motions and strain rate?
  - Over what spatial and frequency ranges?
  - Will shallow heterogeneities and topography have strong effects on spatial gradients?
  - Array processing requires signal coherency across the array.

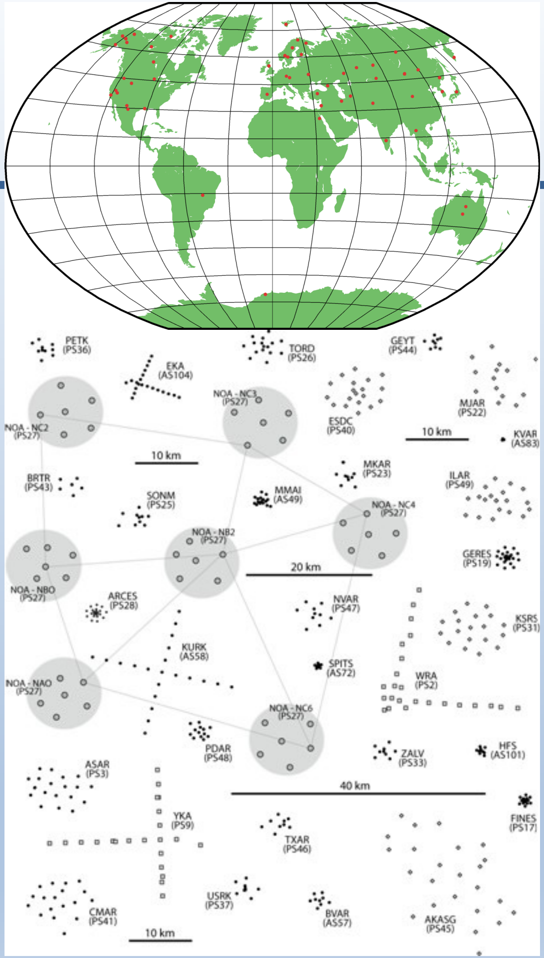

Gibbons (2014)

Data

Earthquakes recorded by PoroTomo Experiment at Brady's Hot Spring (BHS)

Earthquake Source Parameters [1]

Origin-time	Latitude	Longitude	Depth (km)	Mw	ML	Dist[2] (km)	Az[2] (°N)	Baz[2] (°N)	Description
2016-03-19T16:15:39	40.3688	-117.7202	14.2	-	2.9	126	251	60	Winnemucca
2016-03-21T07:37:10	38.4792	-118.3662	9.9	4.01	4.3	157	340	159	Hawthorne
2016-03-22T10:00:45	38.6555	-118.7841	10.9	3.82	4.1	129	352	172	Hawthorne

1. From the Nevada Seismological Laboratory earthquake catalog
2. Distance, Azimuth, and Back-Azimuth between earthquake locations and DAS channel 2000 located at (39.805415°N, 119.004224°W)

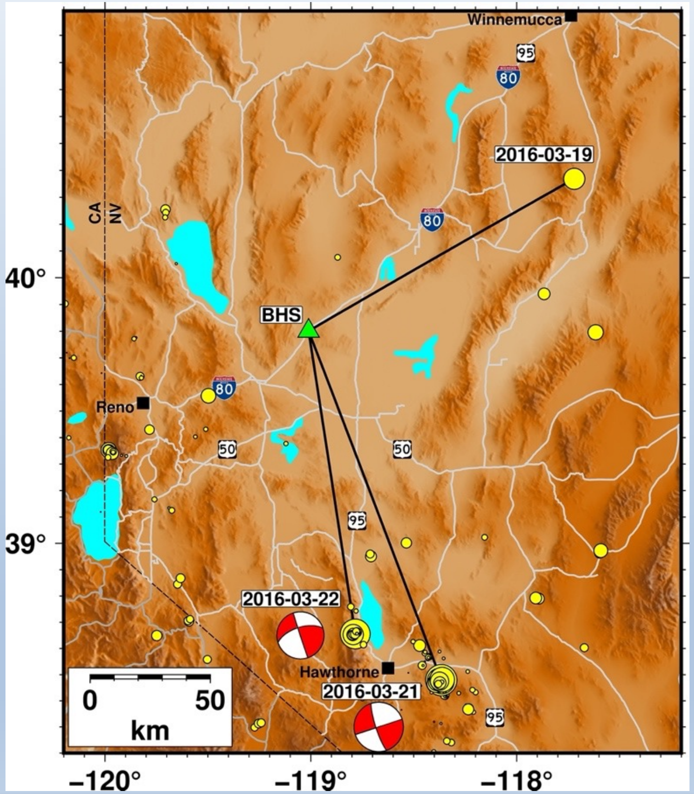

Data

PoroTomo Geophone Large Nodal Array

<u>Geophone Array</u> *(Feigl and Parker, 2019)*

- 242 Fairfield Nodal Z-land 5-Hz 3C geophone sensors
- 1.5 by 1 km area near the injection wells at the Brady Hot Springs geothermal field at an approximate spacing of 60 m

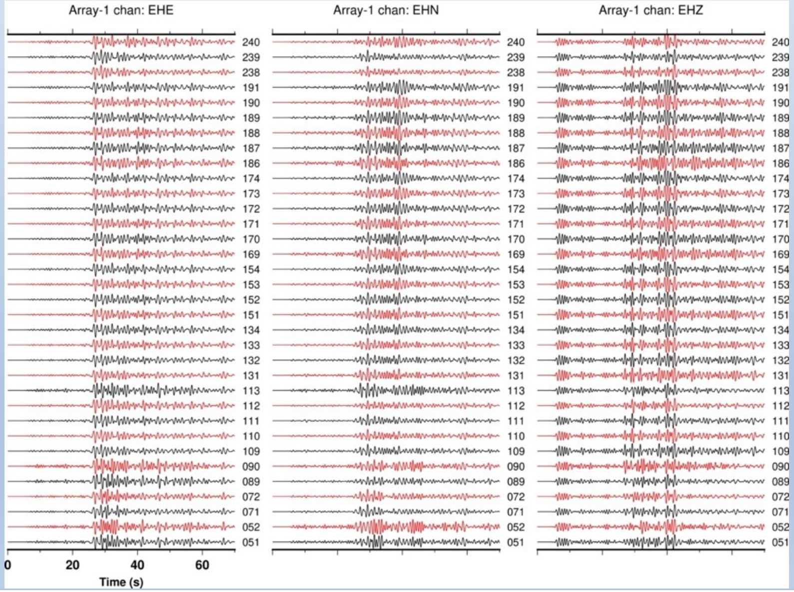

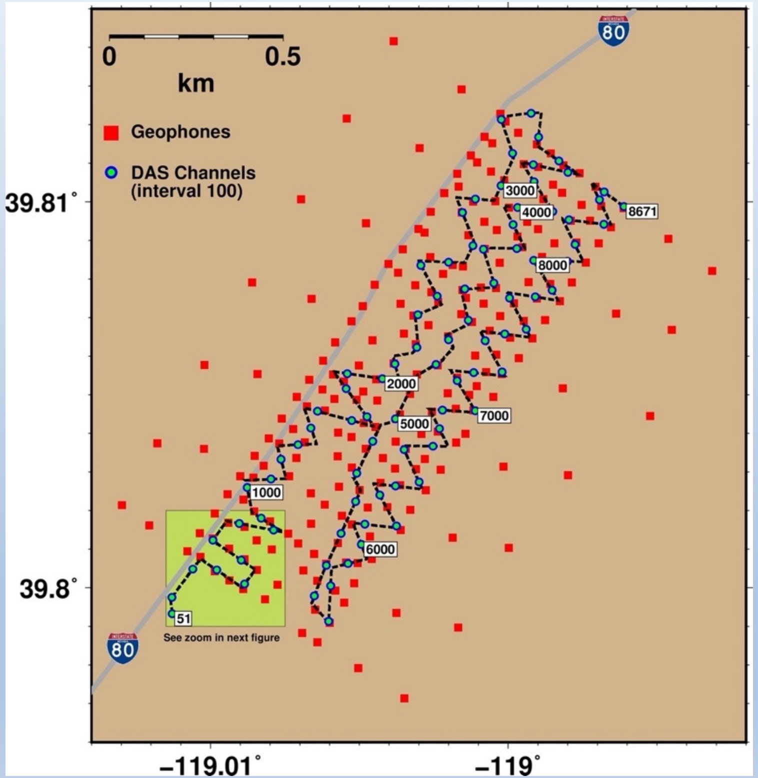

Data

PoroTomo Fiber-optic DAS

<u>**Fiber-optic DAS**</u> *(Feigl and Parker, 2019)*

- Trench was 9 km long, 1 m deep, leveled, and smoothed
- gauge length was set to 10 m based on 100 ns laser pulse width – each channel is 1 meter apart
- 8621 channels
- sampling rate at 1000 samples/sec
- sampling clock was phase locked to a GPS receiver with 1 μsec accuracy
- Channel coordinates determined using tap testing at the cable corners surveyed using high precision GPS to provide fiducial points in UTM coordinates (details in *Wang et al., 2018*).

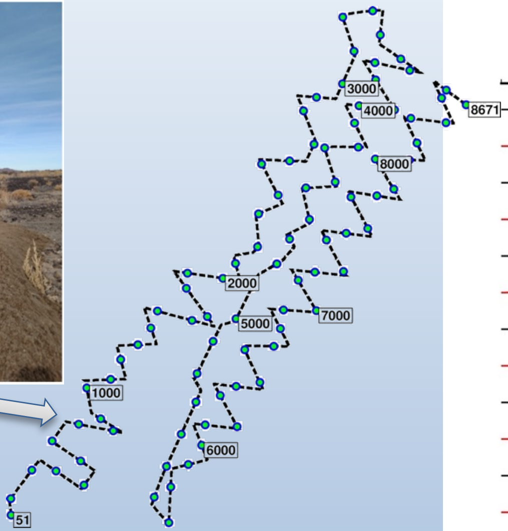

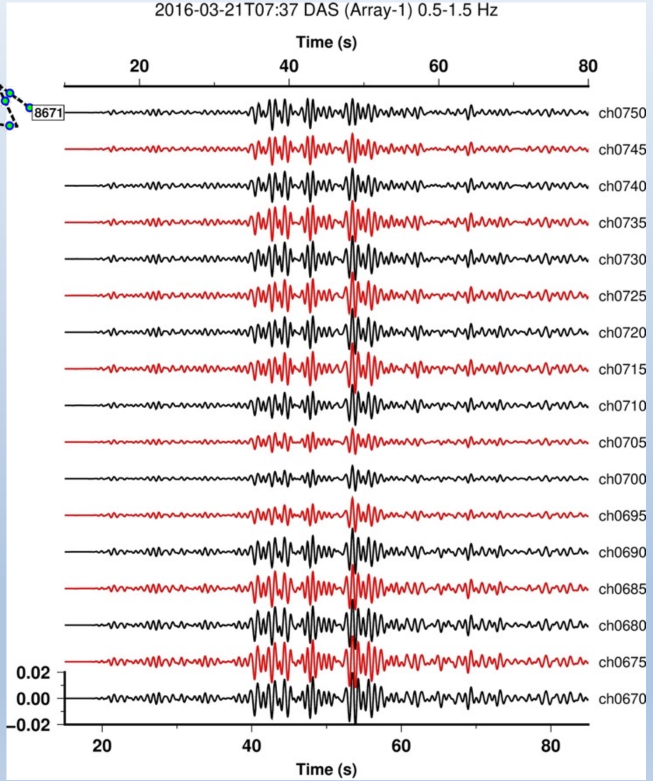

Data

DAS waveform Coherence along fiber-optic cable segment

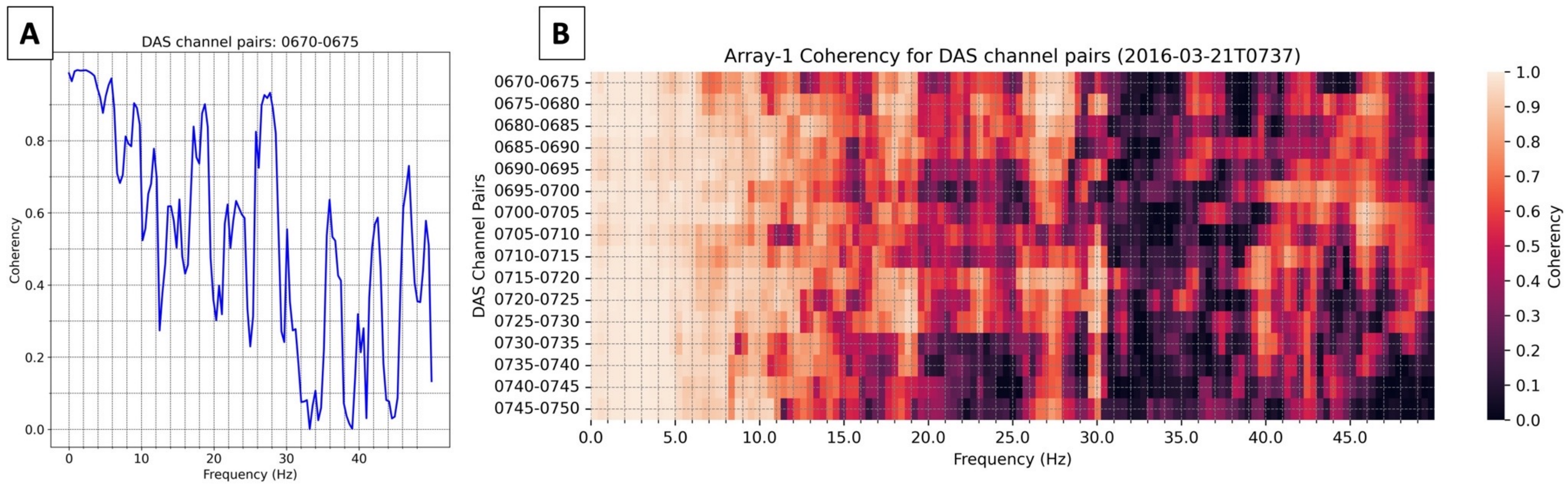

(A) Coherence (scipy.coherence) as a function of frequency from DAS channel pairs 670 and 675 of the 2016-03-21T07:37 Mw 4 Hawthorne earthquake.

(B) Coherency analysis between all 16 DAS channel pairs between channels 670 and 750. High coherence is measured below 6 Hz for channels spaced at least 5 m apart.

Theory and Method

Continuum mechanics, array derived dynamic strain rate, and rotation of strain tensor for axial strain component

$$u(x + \delta x) = u(x) + \boldsymbol{G}\, \delta x$$
$$\boldsymbol{G} = \boldsymbol{\epsilon} + \boldsymbol{\Omega}$$
$$u(x + \delta x) = u(x) + \boldsymbol{\epsilon}\, \delta x + \boldsymbol{\Omega}\, \delta x$$

$$\boldsymbol{d_i^j} = (u_i^j - u_i^0)$$
$$\boldsymbol{R^j} = \left(r^j - r^0\right)$$
$$\boldsymbol{d_i^j} = \boldsymbol{G}\, \boldsymbol{R^j}$$

$where\ (i = x,\ y,\ z)\ component\ and\ jth\ station\ (j = 0)\ reference\ station$

$$u_{z,z} = -\eta(u_{x,x} + u_{y,y}); \qquad \eta = 1 - \left(\frac{2V_S^2}{V_P^2}\right)$$

$$\boldsymbol{G} = \begin{bmatrix} u_{x,x} & u_{x,y} & u_{x,z} \\ u_{y,x} & u_{y,y} & u_{y,z} \\ u_{z,x} & u_{z,y} & -\eta(u_{x,x} + u_{y,y}) \end{bmatrix}$$

$compact\ notation\ u_{x,x} = \partial u_x / \partial x\,,$
$the\ spatial\ gradient\ of\ component\ u_x\ along\ the\ x - axis$

$$\begin{bmatrix} \epsilon_{xx} \\ \epsilon_{yy} \\ \epsilon_{zz} \\ \epsilon_{xy} \\ \epsilon_{xz} \\ \epsilon_{yz} \end{bmatrix} = \begin{bmatrix} u_{x,x} \\ u_{y,y} \\ -\eta(u_{x,x} + u_{y,y}) \\ 1/2\,(u_{x,y} + u_{y,x}) \\ 0 \\ 0 \end{bmatrix}$$

(*e.g., Spudich et al., 1995; Suryanto et al. 2006; Jaeger et al., 2007; Spudich and Fletcher, 2008; Donner et al., 2017*)

The horizontal cartesian components of strain rate $\dot{\epsilon}_{ij}$ can be rotated by angle θ to $\dot{\epsilon}'_{ij}$ using the following transformation matrix,

$$\begin{bmatrix} \dot{\epsilon}'_{xx} \\ \dot{\epsilon}'_{yy} \\ \dot{\epsilon}'_{xy} \end{bmatrix} = \begin{bmatrix} \cos^2\theta & \sin^2\theta & 2\sin\theta\cos\theta \\ \sin^2\theta & \cos^2\theta & -2\sin\theta\cos\theta \\ -\sin\theta\cos\theta & \sin\theta\cos\theta & \cos^2\theta - \sin^2\theta \end{bmatrix} \begin{bmatrix} \dot{\epsilon}_{xx} \\ \dot{\epsilon}_{yy} \\ \dot{\epsilon}_{xy} \end{bmatrix}$$

(*e.g., Jaeger et al., 2007; Donner et al., 2017*)

Array Groups

We created 4 sub arrays within Large-N with varying sizes and aperture lengths

Geophone Array Groups and Fiber-optic DAS Channels Segment Subsets

Array Group	# Geophones	Aperture [1] (m)	# DAS Channels	DAS Segment Length (m)	DAS Channel Range	DAS Segment Azimuth (°N)
1	34	478	17	85	670 - 750	101
2	24	323	29	145	1860 - 2000	97
3	33	389	19	95	2955 - 3045	56
4	24	357	64	320	5265 - 5580	23

[1] *Aperture is maximum distance between geophones in array group*

Frequency bands in Hz = (
0.2 – 0.5,
0.5 – 1.0,
0.5 – 1.5,
1.0 – 2.0,
2.0 – 4.0,
4.0 – 6.0)

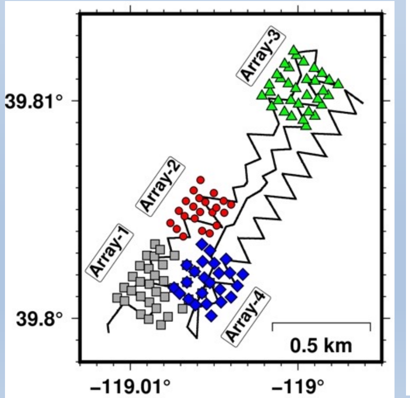

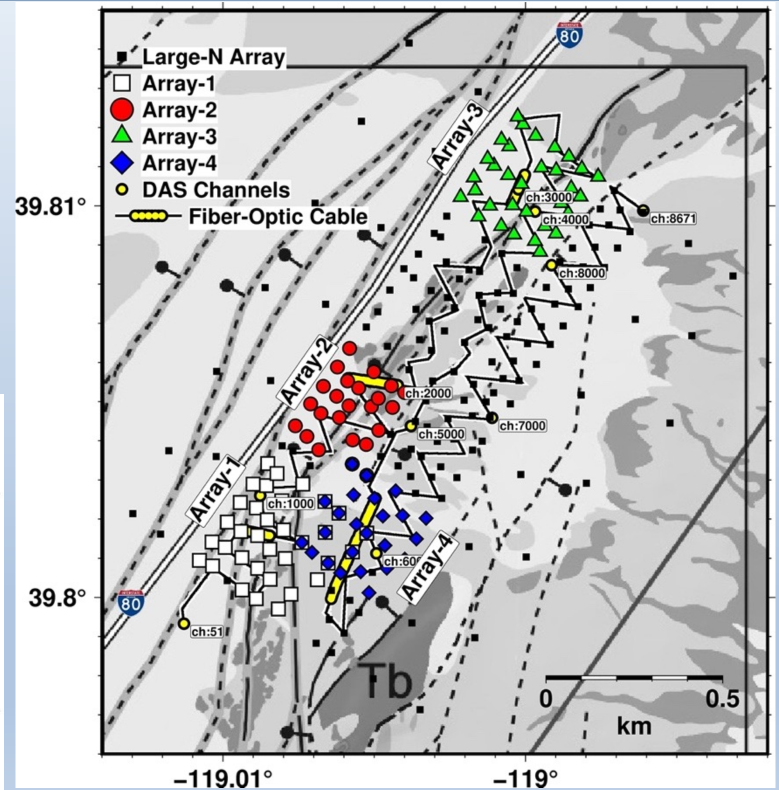

DAS vs. ADDS Comparison Results

ml 2.9 Winnemucca earthquake (0.5-1.5 Hz)

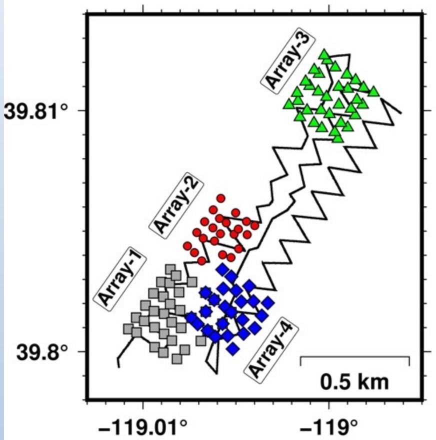

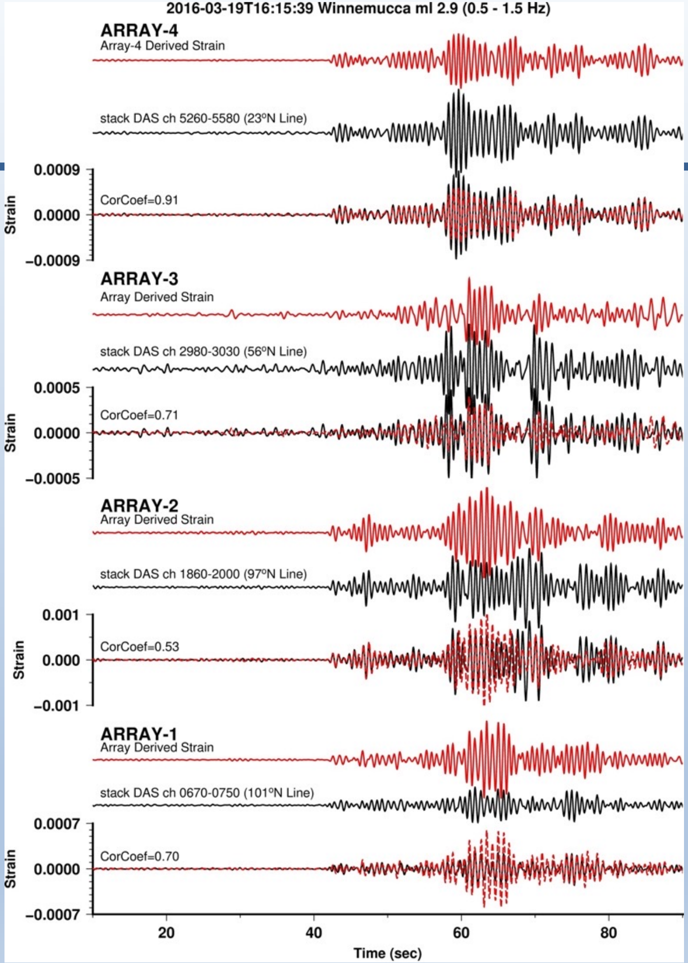

1. lower magnitude, lower SNR
2. Lower coherency Arrays-1, 2, and 3 (S-waves)
3. Higher coherency Array-4 (P- and S-waves)

DAS vs. ADDS Comparison Results

ml 4.1 Hawthorne earthquake (0.5 - 1.5 Hz)

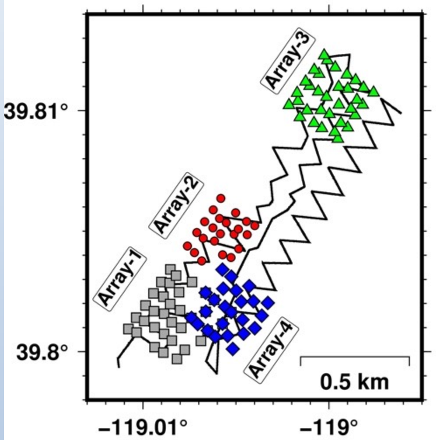

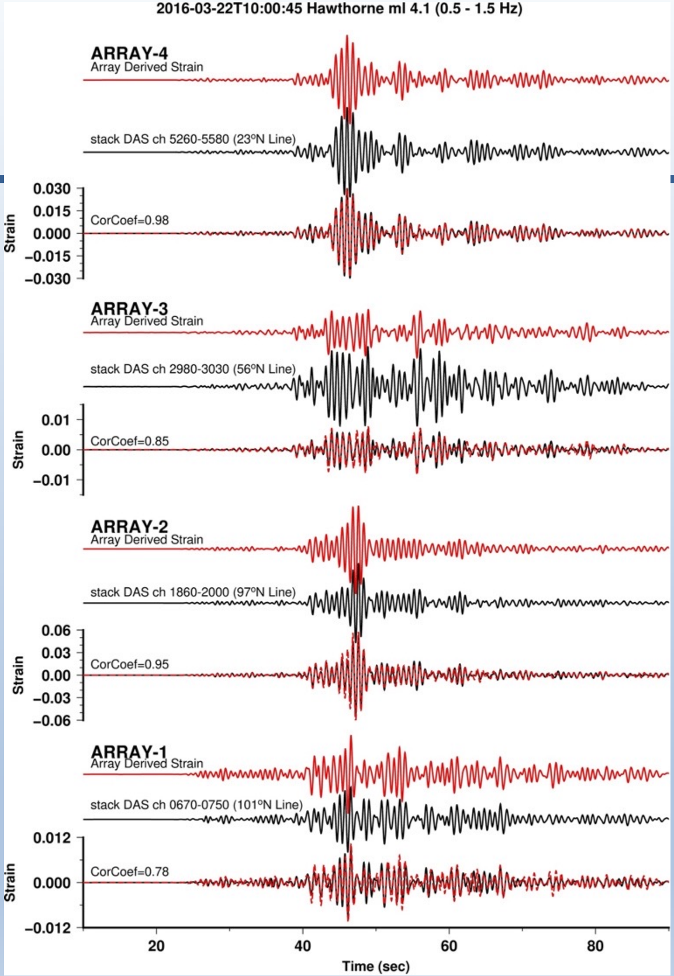

1. Generally, higher coherency for all arrays > 0.78 (P- and S-waves)
2. Array-3 DAS amplitudes 2-times larger than ADDS
3. Similar coherency to previous ml 4.3

Summary of Results

Phase coherency

1. Coherency is highest around 1 Hz, decays quickly with increasing frequency

2. Array-2 and Array-4 more coherent likely due to longer DAS segments

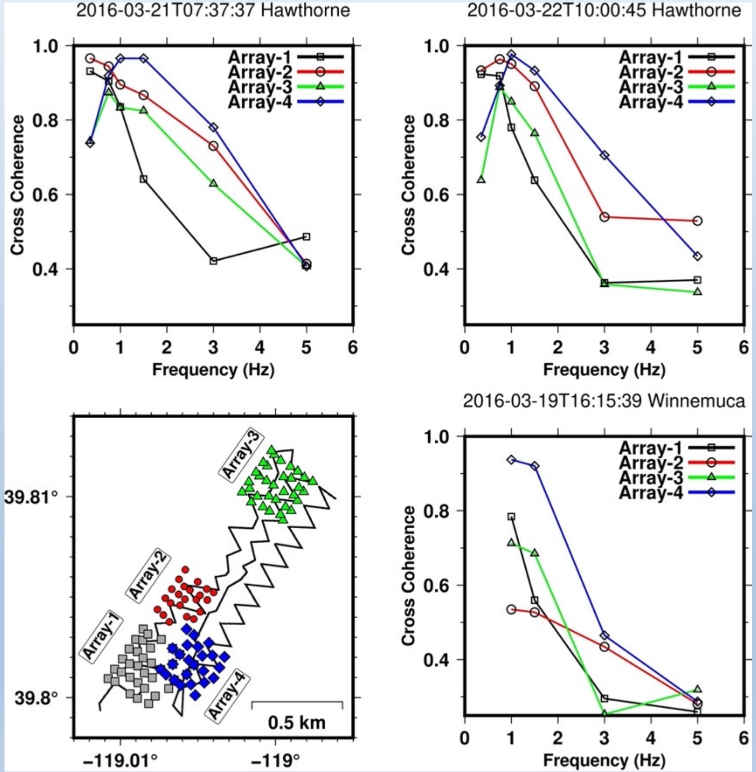

Array Group	# Geophones	Aperture (1) (m)	# DAS Channels	DAS Segment Length (m)	DAS Channel Range	DAS Segment Azimuth (°N)
1	34	478	17	85	670 - 750	101
2	24	323	29	145	1860 - 2000	97
3	33	389	19	95	2955 - 3045	56
4	24	357	64	320	5265 - 5580	23

Summary of Results

RMS amplitude ratios

1. RMS amplitude ratios 0.2-1.5 Hz range between 0.5 -1.5
2. Then increase with frequency to ratios of 2 - 4
3. RMS amplitude ratios smaller for Array-4 and Array-2 (which were also had higher coherency)
4. Amplitudes with SNR < 2 were not used; smaller ml 2.9.

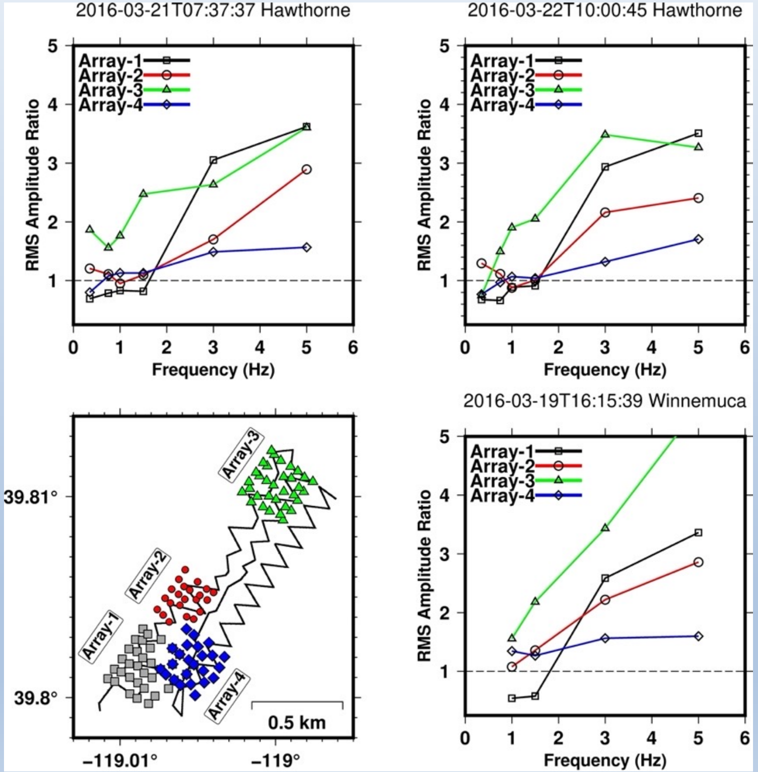

Array Group	# Geophones	Aperture [1] (m)	# DAS Channels	DAS Segment Length (m)	DAS Channel Range	DAS Segment Azimuth (°N)
1	34	478	17	85	670 - 750	101
2	24	323	29	145	1860 - 2000	97
3	33	389	19	95	2955 - 3045	56
4	24	357	64	320	5265 - 5580	23

Conclusions

- We confirm with using ADDS that DAS is measuring axial strain rate.
- ADDS and DAS strain rates compare with high coherency at and below 1 Hz. RMS amplitude ratios are in the 0.5 to 1.5 range below 1 Hz.
- For frequencies greater than 1 Hz, this coherency between ADDS and DAS strain rate decays quickly, below 0.4 and 0.6 correlation for frequencies between 2 and 6 Hz.
- The RMS amplitudes ratios increase with frequency, increasing to ratios of 2 to 4 above 2 Hz. To summarize the points above, array and axial strain rates are only the same around 1 Hz and becomes very frequency dependent above 1 Hz.
- Strains, which are dependent on the spatial gradients, are more sensitive to shallow subsurface geology than particle motions. This could present limitations with seismic analysis methods based on particle motions. For example, array analysis requires coherency between elements. Methods that measure magnitudes from direct phases or coda, that don't require frequency dependent site effects, may not be transportable.

Lawrence Livermore National Laboratory

Data

Data Quality Assessment: Phase changes at cable corners

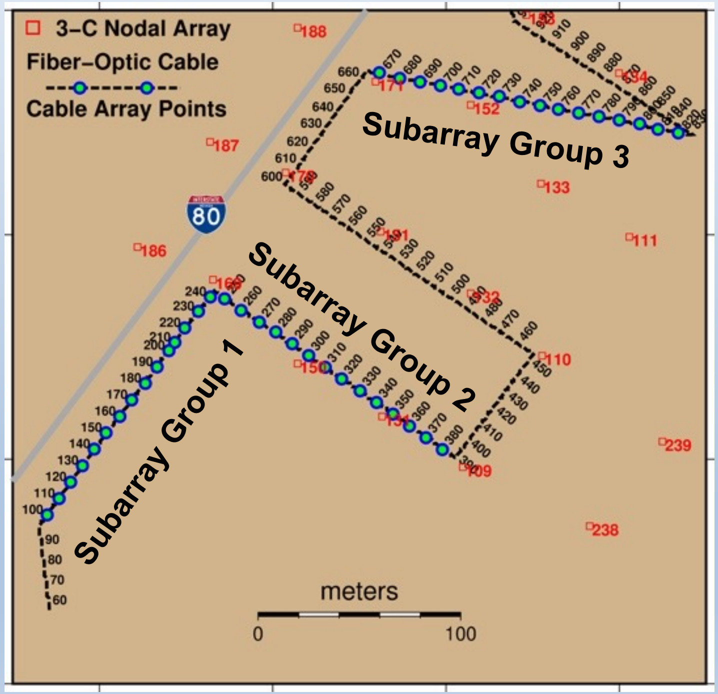

S-wave polarity & amplitude changes at cable corners:
450-460
380-390
240-250
090-100

Problem at 210?

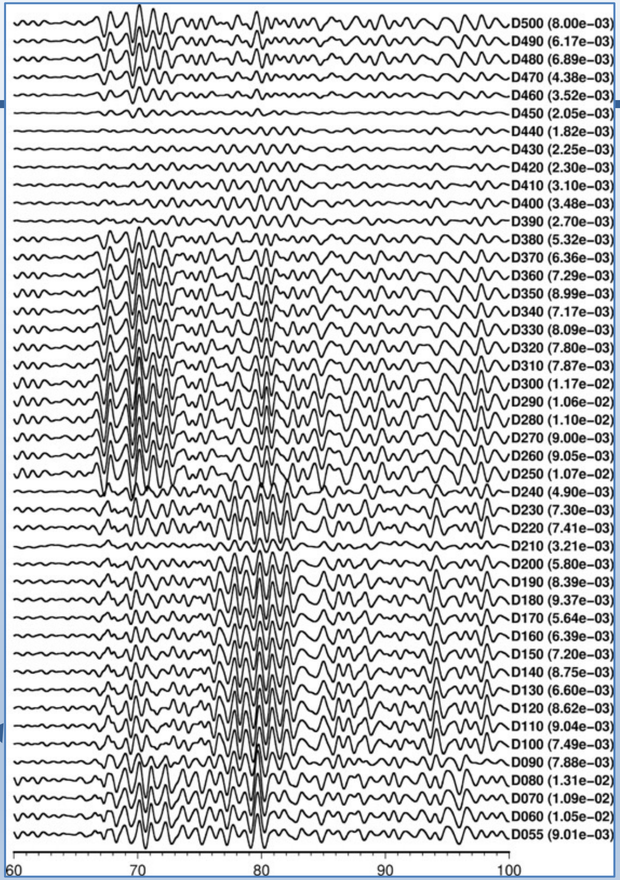

DAS vs. ADDS Comparison Results

ml 4.3 Hawthorne earthquake (0.5 - 1.5 Hz)

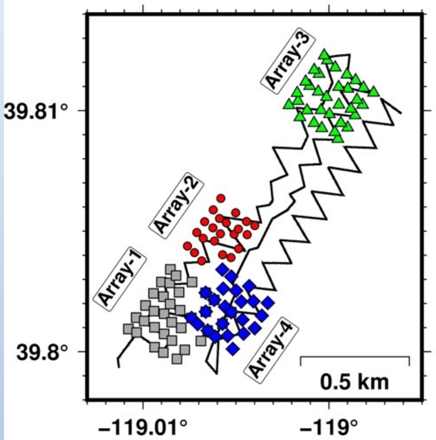

1. Generally, higher coherency for all arrays > 0.83 (P- and S-waves)

2. Array-3 DAS amplitudes 2-times larger than ADDS